Cellular/Molecular

Cytoskeleton Regulation of Glycine Receptor Number at Synapses and Diffusion in the Plasma Membrane

Cécile Charrier,[1] Marie-Virginie Ehrensperger,[2] Maxime Dahan,[2] Sabine Lévi,[1] and Antoine Triller[1]

[1]Laboratoire de Biologie Cellulaire de la Synapse, Institut National de la Santé et de la Recherche Médicale, Unité 789, Ecole Normale Supérieure, 75005 Paris, France, and [2]Laboratoire Kastler Brossel, Centre National de la Recherche Scientifique, Unité Mixte de Recherche 8552, Ecole Normale Supérieure and Université Pierre et Marie Curie, 75005 Paris, France

Lateral diffusion of neurotransmitter receptors in and out of synapses has been postulated as a core mechanism for rapid changes in receptor number at synapses during plastic processes. In this study, we have used single particle tracking to investigate how changes in glycine receptor (GlyR) lateral diffusion properties might account for changes in receptor number at synapses after disruption of the cytoskeleton in dissociated spinal cord neurons. We found that pharmacological disruption of F-actin and microtubules decreased the amount of GlyR and gephyrin, the backbone of the inhibitory postsynaptic scaffold, at synapses. F-actin and microtubule disruption increased GlyR exchanges between the synaptic and extrasynaptic membranes and decreased receptor dwell time at synapses. GlyR lateral diffusion was predominantly controlled by microtubules in the extrasynaptic membrane and by actin at synapses. Both diffusion coefficients and confinement at synapses were affected after F-actin disruption. Our results indicate that receptor exchanges between the synaptic and extrasynaptic compartments depend on the properties of both the postsynaptic differentiation and the extrasynaptic membrane. Consequently, GlyR number at synapses may be rapidly modulated by the cytoskeleton through the regulation of lateral diffusion in the plasma membrane and of receptor stabilization at synapses.

Key words: **inhibitory synapses; glycine receptor; lateral diffusion; single particle tracking; cytoskeleton; plasma membrane**

Introduction

The accumulation of neurotransmitter receptors at synaptic sites is thought to result from their interaction with submembrane scaffolding proteins. The number of synaptic receptors is one of the main determinants of synaptic weight, whose fluctuations must be controlled to preserve neuronal homeostasis (Turrigiano and Nelson, 2004). The glycine receptor (GlyR) is the main inhibitory receptor in the spinal cord and controls the excitability of motoneurons. Antisense (Kirsch et al., 1993) and knock-out experiments (Feng et al., 1998) have shown that GlyR accumulation at synapses relies on gephyrin, the core scaffolding protein of inhibitory postsynaptic differentiations (Moss and Smart, 2001). Light has been shed on the mechanisms underlying receptor stabilization at synapses by the observation that, despite the apparent stability of synapses, the various components of the postsynaptic differentiations are constantly renewed over short timescales (Choquet and Triller, 2003). Lateral diffusion of excitatory and inhibitory receptors has been highlighted as a key process in receptor renewal and concentration at synapses by imaging (Dahan et al., 2003; Tardin et al., 2003; Groc et al., 2004) and electrophysiological (Tovar and Westbrook, 2002; Adesnik et al., 2005; Thomas et al., 2005) studies. More specifically, single particle tracking (SPT) experiments have demonstrated that GlyR stabilization by gephyrin clusters is transient (Meier et al., 2001). GlyRs continuously exchange between the synaptic and extrasynaptic membranes, where they respectively diffuse with brownian and confined motion (Dahan et al., 2003). Therefore, the number of receptors at synapses likely depends on both the regulation of diffusion in the plasma membrane and the capacity of synapses to capture receptors.

The cytoskeleton is a good candidate to regulate GlyR lateral dynamics. Previous studies have shown that GlyR and gephyrin postsynaptic levels and cluster size depend on actin and microtubules (Kirsch and Betz, 1995; van Zundert et al., 2004). Moreover, the submembrane skeleton cortex controls the "apparent viscosity" of mammalian plasma membranes (Kusumi et al., 2005). A well accepted hypothesis is that the cytoskeleton cortex hinders protein movements by creating fences below the membrane or by anchoring transmembrane molecules, which then act as obstacles to lateral diffusion (Kusumi and Sako, 1996; Saxton and Jacobson, 1997). In the context of inhibitory synapses, one must stress that many gephyrin partners are cytoskeleton-related proteins. In addition to tubulin (Kirsch et al., 1991), gephyrin interacts with actin-regulating proteins, such as the GDP/GTP exchange factor collybistin (Kins et al., 2000), profilin (Mammoto et al., 1998), and mammalian enabled (Mena)/vasodilator-stimulated phosphoprotein (VASP) (Giesemann et al., 2003).

In this study, we investigated the implication of the cytoskel-

Received April 25, 2006; revised June 14, 2006; accepted June 15, 2006.

This work was supported by grants from Institut de la Recherche sur la Moelle Epinière and from Association Française contre les Myopathies. C.C. is a recipient of a fellowship from Ministère de la Recherche et de la Technologie, France. We thank B. Riveau for help in cell culture and C. Hanus for helpful discussions.

Correspondence should be addressed to Antoine Triller, Laboratoire de Biologie Cellulaire de la Synapse, Institut National de la Santé et de la Recherche Médicale Unité 789, Ecole Normale Supérieure, 46 rue d'Ulm, 75005 Paris, France. E-mail: triller@biologie.ens.fr.

DOI:10.1523/JNEUROSCI.1758-06.2006

 0270-6474/06/268502-10$15.00/0

eton in the regulation of GlyR lateral diffusion in relation to changes in GlyR and gephyrin concentration at synapses. We confirm that pharmacological disruption of either F-actin or microtubules decreases the amounts of GlyR and gephyrin at synapses. Using SPT, we found that cytoskeleton disruption increased GlyR exchanges between the synaptic and extrasynaptic membranes and decreased receptor dwell time at synapses. Lateral diffusion of GlyRs was predominantly controlled by actin inside synapses and by microtubules outside synapses.

Materials and Methods

Cell culture and transfection. Primary cultures of spinal cord neurons were prepared from embryonic Sprague Dawley rats at day 14 as described previously (Levi et al., 1998). Cells were plated at a density of 5×10^4 cells/cm^2 onto 18 mm diameter glass coverslips (Assistent, Winigor, Germany) precoated with 70 μg/ml poly-D,L-ornithine (Sigma, St Louis, MO) and 5% fetal calf serum (Invitrogen, Cergy Pontoise, France). Cultures were maintained in serum-free Neurobasal medium supplemented with B27 (1×), glutamine (2 mM), and antibiotics (Invitrogen) at 36°C in a 5% CO_2 atmosphere for 10–12 d. The medium was changed at 7 d *in vitro* (DIV). Transfections were done 8 d after plating using the Lipofectamine 2000 method (Invitrogen) according to the manufacturer's protocol with 2 μg in 20 mm wells of plasmid DNA. The plasmid encoded a gephyrin (Prior et al., 1992) and Venus-yellow fluorescent protein (Nagai et al., 2002) chimera (Hanus et al., 2006). Cells were imaged 48 h after transfection.

Drug treatment. Actin filaments and microtubules were depolymerized using, respectively, latrunculin A (3 μM; Sigma) and nocodazole (10 μM; Sigma) initially solubilized in DMSO (Sigma). The final concentrations of DMSO were 0.2 and 0.03%, respectively, and had no effect on GlyR lateral diffusion (data not shown). For immunochemistry, drugs were added directly to the culture medium for the indicated duration before fixation. For SPT experiments, cells were preincubated for 50 min with drugs added to the culture medium, and then stained for GlyRs (see below) and imaged in the MEM recording medium containing the appropriate drug, except in "time course" experiments in which the drug was added to the MEM recording medium at the beginning of the recording. The MEM recording medium consisted of phenol red-free minimal essential medium supplemented with glucose (33 mM; Sigma) and HEPES (20 mM), glutamine (2 mM), Na-pyruvate (1 mM), and B27 (1×) from Invitrogen. To test the reversibility of the drug treatments, cells were treated for 1 h with latrunculin or nocodazole, washed, and incubated overnight in the conditioned culture medium without drug.

Immunofluorescence labeling of fixed cells. Cells were fixed for 15 min at room temperature in 4% (w/v) paraformaldehyde (Serva Feinbiochemica, Heidelberg, Germany) in PBS, and permeabilized for 4 min with 0.25% (v/v) Triton X-100. They were then incubated for 30 min at 37°C in 10% (w/v) bovine serum albumin (BSA) (Sigma) in PBS to block nonspecific staining and incubated for 1 h at 37°C with primary antibodies in 3% BSA. After washes with PBS, cells were incubated for 45 min at 37°C in secondary antibodies, washed, and mounted on slides with Vectashield (Vector Laboratories, Burlingame, CA). The primary antibodies used were mouse anti-GlyR α1-subunit (mAb2b; 1.25 μg/ml; Alexis Biochemicals, San Diego, CA), mouse anti-gephyrin (mAb7a; 1.25 μg/ml; Alexis Biochemicals), and rabbit anti-synapsin I (0.2 μg/ml; Chemicon, Hampshire, UK). Secondary antibodies were Cy3-conjugated goat anti-mouse (1.9 μg/ml) and FITC-conjugated goat anti-rabbit (3.75 μg/ml) from Jackson ImmunoResearch (West Grove, PA). Sets of neurons compared for quantitation were fixed and labeled simultaneously.

Fluorescence image acquisition and quantitative analysis. The effects of latrunculin and nocodazole on the synaptic levels of GlyR and gephyrin were quantified by double-labeling experiments of GlyR or gephyrin and synapsin I as synaptic marker. Isolated cells immunoreactive to GlyR or gephyrin were randomly chosen. Images were acquired in 12-bit mode with a Micromax CCD camera (Princeton Instruments, Trenton, NJ) under 100× objective lenses of 1.3 numerical aperture (NA) on a Leica (Nussloch, Germany) DRM upright microscope using MetaView (Meta Imaging, Downingtown, PA). Exposure time was determined on bright untreated cells to avoid pixel saturation. All GlyR or gephyrin images from a given culture were then acquired with the same exposure time. Quantitations were performed using MetaMorph (Meta Imaging). Images were first flat field divided to prevent nonuniformity in illumination, the background was subtracted, and the images were then median-filtered (kernel size, $3 \times 3 \times 1$) to enhance cluster outlines. A user-defined intensity threshold was applied to select clusters and avoid their coalescence. Thresholded synapsin clusters were dilated using a circular morphology filter (2 pixel diameter). For fluorescence intensity measurements, cell bodies were centered in a 780×780 pixel field, and only receptor or gephyrin clusters comprising at least 3 pixels and apposed on at least 1 pixel with a synapsin cluster were considered.

GlyR live-cell staining for single particle imaging. Neurons were incubated for 5 min in mAb2b (0.6–1.25 μg/ml), washed, and incubated for 5 min in biotinylated anti-mouse Fab antibody (0.35–2.8 μg/ml; Jackson ImmunoResearch). After washes, cells were incubated for 1 min in streptavidin-coated quantum dots (QDs) emitting at 605 nm (0.2–0.3 nM; Quantum Dot Corporation, Hayward, CA) in borate buffer (50 mM) supplemented with sucrose (200 mM) and extensively washed. After GlyR labeling, active presynaptic terminals were stained for 30 s with *N*-(3-triethylammoniumpropyl)-4-(6-(4-diethylamino)phenyl)-hexatrienyl)pyridinium dibromide (FM4-64) (2 μM; Invitrogen) in the presence of KCl (40 mM) to stimulate vesicular recycling. Cells were then washed extensively. All incubation steps and washes were performed at 37°C in the MEM recording medium.

Single particle imaging. Neurons were imaged in the MEM recording medium at 37°C in an open chamber mounted onto a IX70 inverted microscope (Olympus, Tokyo, Japan) equipped with a 60× objective (NA, 1.45; Olympus). QDs and FM4-64 were detected using an Hg^+ lamp (excitation filter, 525DF45) and appropriate emission filters (605WB20 and 695AF55, respectively; Omega Filters, Brattleboro, VT). QD real-time recordings were acquired with a CCD camera (Micromax 512EBFT; Princeton Instruments) during 512 consecutive frames with an exposure time of 75 ms using MetaView. GlyR labeled with QDs (GlyR-QDs) were recorded on proximal dendrites of isolated cells randomly chosen with transmission illumination. Cells were imaged within 30 min after GlyR staining. Intracellular GlyR staining was not detected during this time period, as checked by acid wash assays on untreated and treated cells (data not shown) or with immunoelectron microscopy (Dahan et al., 2003), indicating no massive internalization of GlyRs.

Single particle tracking and quantitative analysis. In all quantitations, single QDs were identified by their blinking, that is, the random alternation between an emitting state and a nonemitting state (Alivisatos et al., 2005). GlyR-QD location (synaptic, perisynaptic, or extrasynaptic) was determined by comparison with the FM4-64 image, as described by Dahan et al. (2003).

Diffusion coefficients and confinement at synapses. Diffusion coefficients and size of confinement domains were determined from short trajectories (30–150 frames) during which QDs did not blink and remained in the same compartment. Single QD tracking was performed with homemade software (Matlab; The Mathworks, Natick, MA). The center of the spot fluorescence was determined using a Gaussian fit with a spatial resolution of ~10 nm. Values of the mean square displacement (MSD) were calculated from the trajectories applying the relation: $\mathrm{MSD}(ndt) = (N-n)^{-1}\Sigma_{i=1}^{N-n}((x_{i+n}-x_i)^2 + (y_{i+n}-y_i)^2)$ (Saxton, 1997), where x_i and y_i are the coordinates of an object on frame i, N is the total number of steps in the trajectory, dt is the time interval between two successive frames, and ndt is the time interval over which displacement is averaged. Diffusion coefficients (D) were calculated by fitting the first five points of the MSD curves versus time (t) with the equation $\mathrm{MSD} = 4Dt$. For synaptic trajectories, the size of the domain of confinement was estimated by fitting the convenient MSD with the expected generic expression for a confined diffusion (Kusumi et al., 1993) as follows:

$$\mathrm{MSD}\ (t) = \frac{L^2}{3}\left(1-\exp\left(\frac{-12Dt}{L^2}\right)\right)$$

where L is the side of a square domain in which diffusion is supposed to be restricted. We considered that receptors were confined in circular synaptic areas whose diameter d_{conf} was related to L by

$$d_{conf} = (2/\sqrt{\pi})L.$$

Transitions between synaptic and extrasynaptic compartments and dwell time at synapses.

Because of QD blinking, single GlyR-QD trajectories were reconstructed over the recordings using homemade software (Bonneau et al., 2004). To analyze the reconstructed trajectories, the synaptic compartment was extended to the perisynaptic area so that GlyR-QDs could be detected in three states: synaptic (state 1), extrasynaptic (state 0), and nonemitting (state −1). The state of single GlyR-QDs was plotted over time (see also Fig. 6*A*). Then, GlyR-QD location during nonemitting events was approximated as follows. When GlyR-QD was detected in the same compartment before and after the nonemitting event, we considered that GlyR-QD remained in the same compartment and the duration of the nonemitting event was added to the time spent in this compartment. When GlyR-QD was not detected in the same compartment before and after the nonemitting event, we considered that one transition occurred during this time period and the duration of the nonemitting event was equally shared between the two compartments. After this time reallocation, transitions between states 0 and 1 were filtered to avoid overestimating their number. This processing introduced a variation <2.6% in the time spent in each compartment, independently of the pharmacological treatment. The number of transitions was calculated for each recording by dividing the sum of entries and exits of synapses by the number of GlyR-QDs in the field and by the total duration of GlyR-QDs detection. Dwell time at synapses was defined as the duration of detection of GlyR-QDs at synapses on a recording divided by the number of exits from synapses.

Statistical analysis and image preparation. Statistical analyses were done using StatView (Abacus Concepts, Berkeley, CA) on data compiled and analyzed using Microsoft Excel (Microsoft, Les Ulis, France). Images were prepared for printing using Photoshop and Illustrator (Adobe Systems, San Jose, CA).

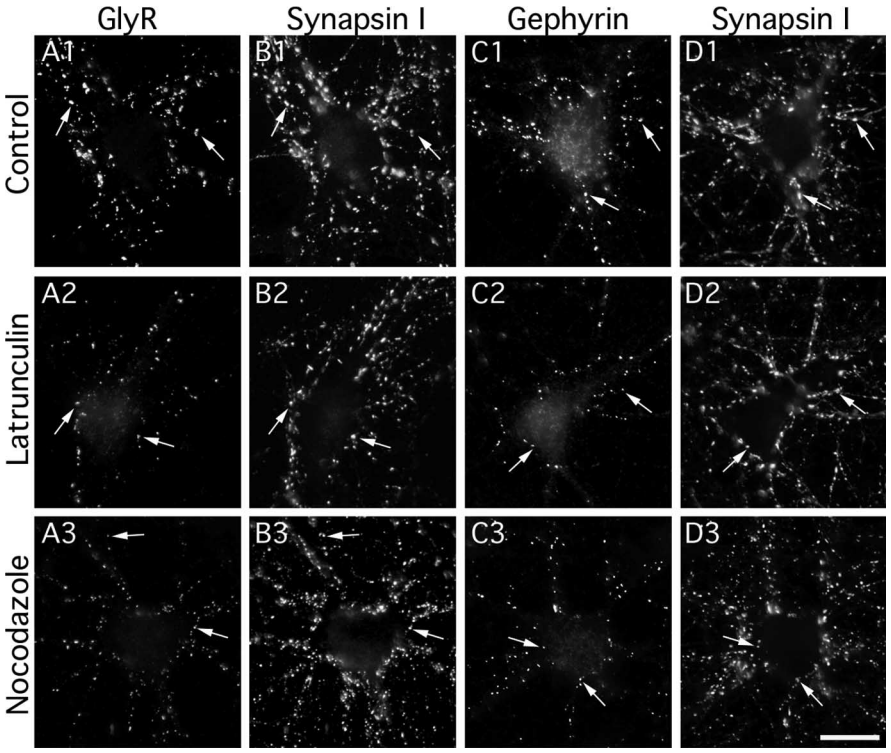

Figure 1. Effects of F-actin and microtubule disruption on GlyR and gephyrin clusters. Double detection of GlyR (***A***) and synapsin (***B***) or gephyrin (***C***) and synapsin (***D***) in cultured spinal cord neurons (10–12 DIV). GlyR (***A1–A3***) and gephyrin (***C1–C3***) formed aggregates (arrows) apposed to presynaptic terminals (***B1–B3*** and ***D1–D3***, respectively) in control conditions (***A1–D1***) or after 1 h treatment with 3 μM latrunculin (***A2–D2***) or 10 μM nocodazole (***A3–D3***). Note that GlyR-, gephyrin-, but not synapsin-associated immunoreactivity decreased in the presence of latrunculin or nocodazole. Scale bar, 20 μm.

Results

The involvement of the cytoskeleton in GlyR lateral dynamics was studied using a pharmacological approach in 10–12 DIV spinal cord neurons. At this age, cultured spinal cord neurons form biochemically "mature" synaptic contacts (Ransom et al., 1977). F-actin and microtubules were disrupted using the depolymerizing agents latrunculin A (Lat) (3 μM) and nocodazole (Nz) (10 μM), respectively. Immunofluorescence experiments were used to establish the efficiency and reversibility of drug application protocols, thus also ensuring their compatibility with neuron survival. We analyzed the GlyR α1-subunit, the predominant adult GlyR α-subunit isoform (Becker et al., 1988).

Cytoskeleton disruption and GlyR and gephyrin levels at synapses

GlyR and gephyrin levels at synapses were quantified using immunocytochemistry on fixed cells. In control conditions, GlyRs (Fig. 1*A1*) and gephyrin (Fig. 1*C1*) formed clusters apposed to presynaptic terminals identified with synapsin I immunofluorescence (Fig. 1*B1*,*D1*, respectively). After 1 h of treatment with latrunculin or nocodazole, GlyR and gephyrin clusters were smaller and less fluorescent, but still apposed to presynaptic terminals (Fig. 1*A2*,*B2*;*A3*,*B3*, respectively, for GlyR; and *C2*,*D2*; *C3*,*D3*, respectively, for gephyrin). Synapsin I immunofluorescence was not modified after latrunculin (Fig. 1*B2*,*D2*) or nocodazole (Fig. 1*B3*,*D3*) treatments, consistent with the notion that maintenance of presynaptic proteins is independent of F-actin and microtubule integrity (Kirsch and Betz, 1995; Allison et al., 1998; Zhang and Benson, 2001; van Zundert et al., 2004). GlyR and gephyrin levels at synapses were quantified by measuring the integrated fluorescence intensity associated with the postsynaptic clusters. After 1 h of latrunculin or nocodazole treatment, GlyR-associated fluorescence at synapses was 48 ± 4 and 58 ± 4%, respectively, of the fluorescence measured in control conditions (Fig. 2*A1*) ($n_{Ctr} = 79$; $n_{Lat} = 48$; $n_{Nz} = 46$; from at least three independent cultures; $p < 10^{-4}$, ANOVA, PLSD test). Gephyrin-associated fluorescence at synapses was 59 ± 3 and 69 ± 3%, respectively, of the fluorescence measured in control conditions after the same treatments (Fig. 2*A2*) ($n_{Ctr} = 63$; $n_{Lat} = 46$; $n_{Nz} = 43$; from at least three independent cultures; $p < 10^{-4}$, ANOVA, PLSD test). In line with previous reports (Kirsch et al., 1995; van Zundert et al., 2004), these results demonstrate that GlyR and gephyrin levels at synapses depend on actin and microtubule cytoskeleton integrity.

We then analyzed the time course of latrunculin- and nocodazole-induced decreases in GlyR- and gephyrin-associated fluorescence at synapses. For normalization, the effect of treatments was expressed as a percentage of the maximal effect, as seen

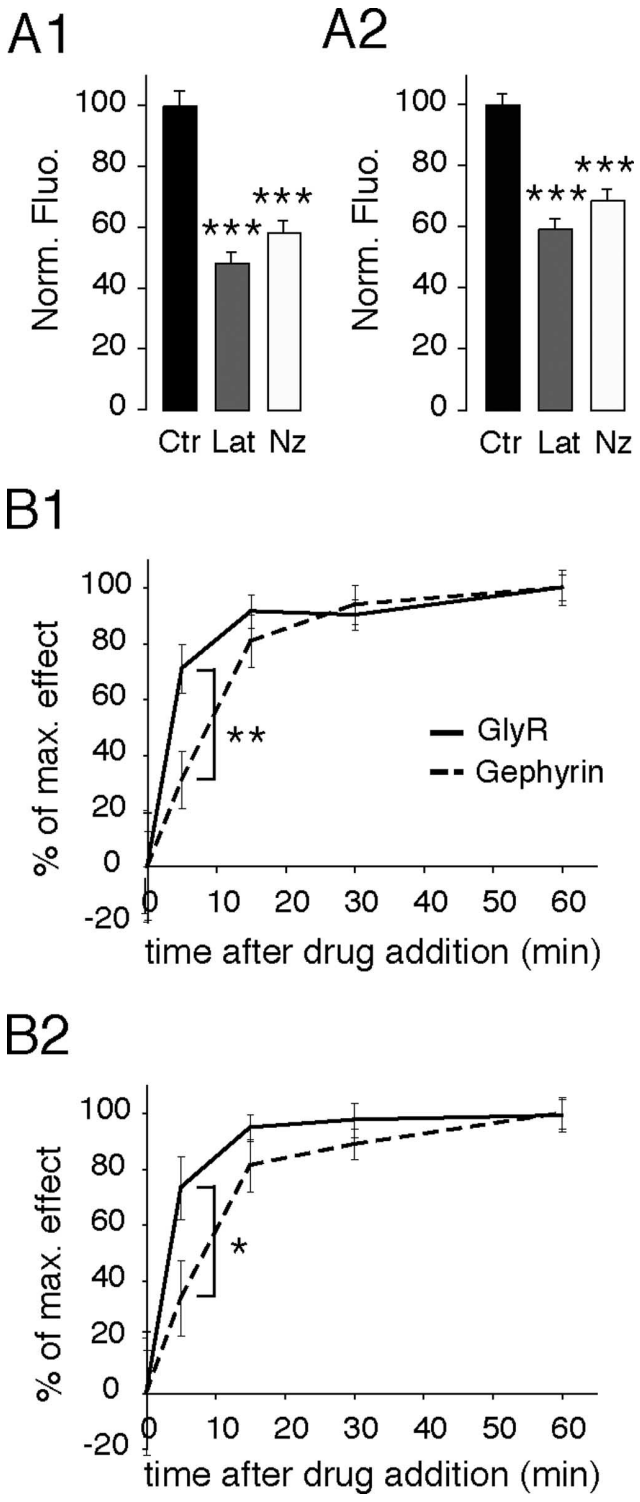

Figure 2. Decrease of GlyR- and gephyrin-associated fluorescence at synapses after F-actin and microtubule disruption. ***A***, Normalized intensity of GlyR- (***A1***) and gephyrin- (***A2***) associated fluorescence at synapses, expressed as percentage of control, in control conditions (Ctr) (black), or after 1 h treatment with Lat (gray) or Nz (white). GlyR- and gephyrin-associated fluorescence significantly decreased in the presence of latrunculin or nocodazole. Values are averages ± SEM. ***$p < 10^{-4}$, ANOVA, PLSD test. ***B***, Time course of latrunculin (***B1***) and nocodazole (***B2***) effects on GlyR (full line) and gephyrin (dashed line) synaptic cluster fluorescence intensity. The effects of latrunculin and nocodazole treatments on GlyR-associated fluorescence precede those on gephyrin. Values (mean ± SEM) are expressed as the percentage of the maximum effect. In all cases, 18–23 cells from two independent cultures were analyzed 0, 5, 15, 30, and 60 min after the addition of the drug. *$p < 5 \times 10^{-2}$, **$p < 10^{-2}$, Mann–Whitney test.

after 1 h of treatment. GlyR- and gephyrin-associated fluorescence decline leveled off ~15 min after the addition of latrunculin or nocodazole (Fig. 2*B1*,*B2*, respectively). This indicates that, between 15 and 60 min of latrunculin and nocodazole treatment, a subpopulation of molecules remains insensitive to actin and microtubule disruption. GlyR-associated fluorescence decreased sharply to 71 and 73% of the maximal effect after only 5 min of treatment with latrunculin or nocodazole (Lat, $p < 10^{-3}$; Nz, $p < 10^{-2}$; Mann–Whitney test) (Fig. 2*B1*,*B2*, respectively). This indicates that cytoskeleton disruption induces rapid variations in GlyR number at synapses. Gephyrin-associated fluorescence decreased to 31 and 34% of the maximal effect after 5 min of the latrunculin and nocodazole treatments, respectively. Therefore, the observed nocodazole and latrunculin effects on gephyrin occurred slower than those seen for GlyR. Indeed, we cannot exclude that this delay was attributable to differences in immunoreactivity, or to limits in the detection of the fluorescence. However, fluorescence was detected using a high dynamic range camera (see Materials and Methods) and the GlyR- and gephyrin-associated fluorescence was far from the background noise of the preparation.

Antibody binding experiments on living cells followed by an acid wash (pH 2; 4 min) indicated that endocytosis was not responsible for the decrease in GlyR-associated fluorescence at synapses (data not shown). In line with previous experiments (Kirsch and Betz, 1995), this favors the notion that GlyRs rapidly spread in the extrasynaptic membrane after cytoskeleton disruption, and suggests that actin and microtubules control the previously demonstrated (Dahan et al., 2003) lateral diffusion of GlyRs in the somatodendritic membrane.

Effects of F-actin and microtubule disruption on GlyR lateral diffusion

Actin and microtubule involvement in GlyR lateral diffusion was analyzed using SPT. Endogenous GlyRs were immunodetected with low concentrations of antibodies using QDs as fluorescent probe. QDs allow the tracking of GlyRs (GlyR-QD) in and out of synapses for long durations with a high precision of localization (≈10 nm) (Dahan et al., 2003). Active presynaptic terminals were stained with FM4-64. GlyRs were tracked in 13 Hz recordings. Single QDs were identified thanks to their blinking (Alivisatos et al., 2005). In control conditions, as seen on a sequence (Fig. 3*A1–A3*; supplemental movie 1, available at www.jneurosci.org as supplemental material) and better viewed on the projection (Fig. 3*B*), GlyR-QDs displayed various diffusive behaviors. They could be mobile (purple symbols, elongated trajectories on the projection) over extrasynaptic portions of the membrane, or more stable (green symbols, circular trajectories on the projection) at synapses. GlyR-QDs could also exchange between the synaptic and extrasynaptic membranes (not shown in this example) in agreement with previous observations (Dahan et al., 2003). In the presence of latrunculin, GlyR-QDs tended to diffuse over broader areas. GlyR-QDs were more frequently found to exchange between the synaptic and extrasynaptic membranes (Fig. 3*C*,*D*, yellow arrowheads; supplemental movie 2, available at www.jneurosci.org as supplemental material) and to swap from one synapse to another (Fig. 3*C*,*D*, yellow arrows). In the presence of nocodazole, receptor diffusion was dramatically increased. Large surface areas of the extrasynaptic membrane were explored during the recording sessions, and GlyR-QDs were frequently seen passing through synapses (Fig. 3*E*,*F*, yellow symbols; supplemental movie 3, available at www.jneurosci.org as supplemental material). Stable receptors at synapses

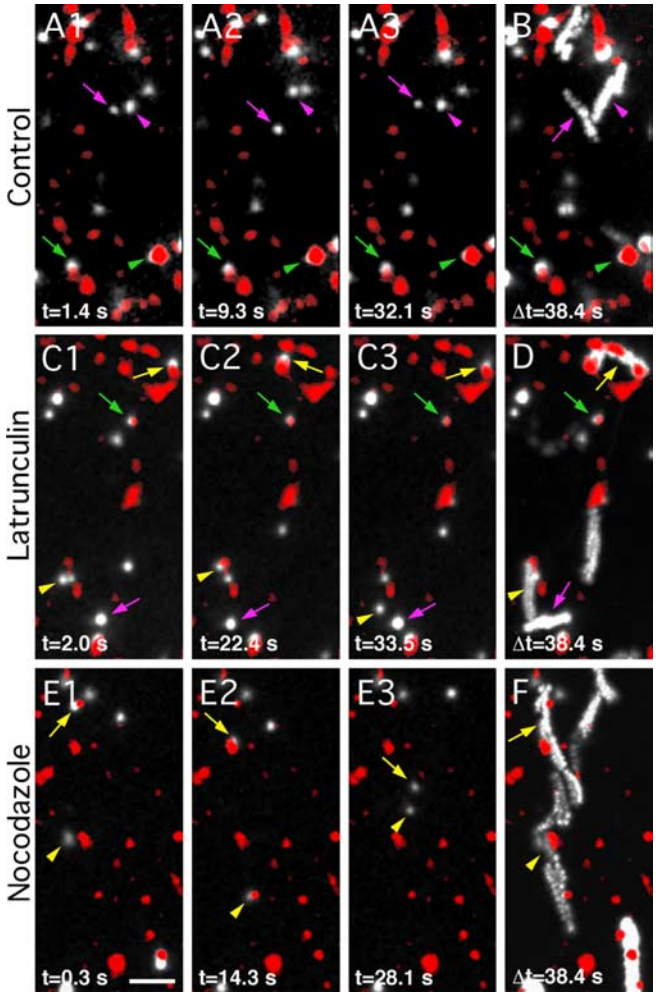

Figure 3. Effects of F-actin or microtubule disruption on GlyR lateral diffusion. Examples of GlyR SPT recordings in cultured spinal cord neurons (10–12 DIV) in control conditions (***A***, ***B***), or after 1 h incubation with latrunculin (***C***, ***D***) or nocodazole (***E***, ***F***). Active presynaptic terminals were labeled with FM4-64 (red). GlyRs were immunodetected with QDs (GlyR-QDs) (white). ***A1–A3***, ***C1–C3***, ***E1–E3***, Sequences of pictures extracted from a recording at the indicated times. ***B***, ***D***, ***F***, Maximum intensity projections emphasizing the surface area explored by GlyR-QDs during a 38.4 s recording sequence. Note the differences in the explored surface area and the transitions between synaptic and extrasynaptic compartments in control, latrunculin, and nocodazole conditions. Symbols: arrows, arrowheads, and crossed arrows are for identified GlyR-QDs; colors: green and purple, synaptic and extrasynaptic GlyR-QDs, respectively; yellow, GlyR-QDs swapping between the synaptic and extrasynaptic compartments. Scale bar, 5 μm.

were rarely found after microtubule disruption. This shows that actin and microtubules control lateral diffusion of GlyRs.

In the presence of latrunculin and nocodazole, GlyR-QDs explored large portions of dendrites. During their journey in the plasma membrane, they passed through different landscapes including surfaces associated with FM4-64 staining. The consequence of the presence of a synaptic bouton on a receptor trajectory was evaluated using diffusion coefficient measurements (Dahan et al., 2003). In the examples illustrated in Figure 4, we have selected trajectories with rapid motions and which were associated only for short periods of time with FM4-64-stained profiles (Fig. 4*A1*, example in the presence of latrunculin; *A2*, example in the presence of nocodazole). The averaged diffusion coefficients of GlyR-QDs were determined over continuous periods, the duration of which corresponded to the presence of a GlyR-QD in the synaptic compartment (i.e., apposed to FM4-64 staining) or out of synapses (i.e., not apposed to FM4-64 staining). In the presence of latrunculin (Fig. 4*B1*) or nocodazole (Fig. 4*B2*), the diffusion coefficients were consistently slower when the GlyR-QDs were associated with labeled synaptic boutons. This supported the notion that, on these trajectories, stretches associated with FM4-64 staining corresponded to passages in the synaptic membrane, and not to diffusion on other bundled dendrites.

We then questioned whether changes in GlyR diffusive behavior at synapses occurred at inhibitory synapses. SPT experiments were performed on neurons transfected with a fluorescent gephyrin chimera. A Venus-tagged gephyrin (Vege) was used to visualize inhibitory postsynaptic structures. As previously demonstrated, almost all endogenous synaptic gephyrin clusters contain the fluorescent chimera 24–48 h after transfection in cultured spinal cord neurons (Hanus et al., 2006). In our experiments, the codetection of FM4-64 and Vege allowed identification of inhibitory synapses. As illustrated in a latrunculin experiment (Fig. 5), GlyR-QDs could exhibit various behaviors. Some GlyR-QDs diffused rapidly through inhibitory synapses and swapped from a synaptic Vege cluster to another one (Fig. 5, GlyR-QD 1). Other GlyR-QDs remained stable at Vege clusters (Fig. 5, GlyR-QD 2) or were mobile in the extrasynaptic membrane (Fig. 5, GlyR-QD 3). GlyR-QDs were also detected at synapses not labeled by a Vege cluster (Fig. 5, GlyR-QDs 1 and 4). These synaptic contacts could (1) be located on dendrites from nontransfected neurons; (2) correspond to excitatory synaptic contacts, which represent 35% of synaptic contacts in comparable cultured spinal cord neurons (Dumoulin et al., 1999); and (3) correspond to inhibitory synapses, which, although on a transfected neuron, were not colonized by the venus::gephyrin chimera. Despite the rapid motion of GlyR-QD 1, the instantaneous diffusion coefficients slowed down during passages through gephyrin clusters at inhibitory synapses (Fig. 5*C*), which is consistent with previous observations (Meier et al., 2001).

Together, these results demonstrate that the rapid diffusion of GlyRs through synapses observed after cytoskeleton disruption occurs at inhibitory synapses.

Effect of cytoskeleton disruption on exchange of GlyRs between the synaptic and extrasynaptic compartments and dwell time at synapses

Although the relationship between receptor lateral diffusion and local concentration at synapses has not been established, it is implicit through the concept of stabilization. Stabilization of receptors at synapses, which is responsible for receptor local concentration, is related to receptor dwell time (that is, to the probability that a receptor leaves a synapse once it has entered it). In this section, we have analyzed the effects of latrunculin and nocodazole treatments on the number of receptor transitions between the synaptic and extrasynaptic compartments and on receptor dwell time at synapses. Quantification of these parameters required the determination of GlyR-QD location throughout the recording despite QD blinking. After reconstruction of the trajectories, we plotted the state of each GlyR-QD (synaptic, 1; extrasynaptic, 0; blink, −1) as a function of time (Fig. 6*A1*). We then approximated the behavior of the GlyR-QDs during the blinking events. Because transitions between the synaptic and extrasynaptic compartments were not frequent in control recording sessions, we considered that there was either one transition (Fig. 6*A*, purple stars) or none (Fig. 6*A*, black stars) between the synaptic and extrasynaptic compartments depending on GlyR-QD location before and after a blinking event, and time was then reallocated to each compartment (see Materials and Meth-

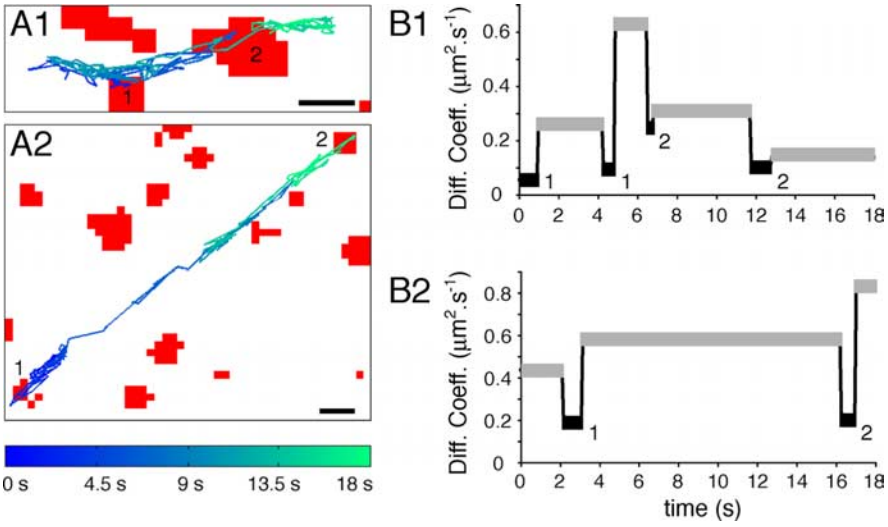

Figure 4. Decrease in GlyR diffusion coefficients at synapses independently of cytoskeleton-disrupting treatments. ***A***, Reconstruction of 18 s GlyR-QD mass center trajectory over the FM4-64-stained synapses (red) images after 1 h treatment with latrunculin (***A1***) or nocodazole (***A2***). Scale bars, 1 μm. ***B***, Comparison of diffusion coefficients averaged during extrasynaptic (gray) and synaptic (black) sequences from the trajectory illustrated in ***A*** in latrunculin (***B1***) or nocodazole (***B2***) condition. Numbers correspond to synapses in ***A***. Note that, despite the latrunculin- and nocodazole-induced increase in GlyR lateral mobility, receptors are consistently slowed down at synapses.

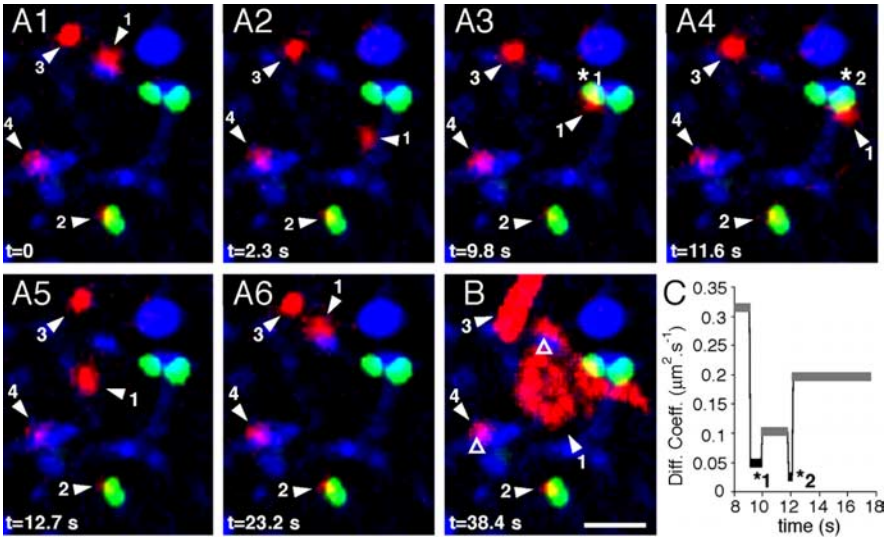

Figure 5. GlyR lateral diffusion at inhibitory synapses. Example of a recording session of GlyR-QDs on neurons transfected with Vege chimera in the presence of latrunculin. Blue, FM4-64-stained synapses; red, GlyR-QDs; green, Vege-containing inhibitory postsynaptic microdomains. ***A1–A6***, Sequence of pictures extracted from a 38.4 s recording session at the indicated times. ***B***, Maximum intensity projection showing the surface area explored by GlyR-QDs during the recording session. Various diffusive behaviors are found in this field. GlyR-QD 1 swaps between a Vege-devoid synapse (***B***, open triangle) and Vege-containing synapses (***A3***, star 1; ***A4***, star 2). GlyR-QD 2 remains at the same Vege cluster. GlyR-QD 3 and 4 are mobile in the extrasynaptic membrane and stable at a Vege-devoid synapse (***B***, open triangle), respectively. Scale bar, 2 μm. ***C***, Averaged diffusion coefficients of GlyR-QD 1 during extrasynaptic (gray) and synaptic (black) sequences.

ods). GlyR-QDs could then be classified in two states: extrasynaptic, 0; or synaptic, 1 (Fig. 6*A2*). Subsequently, the location of GlyR-QDs as a function of time was filtered (Fig. 6*A3*) to avoid an overestimation of the exchanges between the compartments (Fig. 6*A*, red circles). Overestimation may result from the lower resolution of FM4-64 fluorescence detection (pixel edges) compared with the pointing accuracy of QDs (≈10 nm, independent of pixel size) (see Materials and Methods), which creates a background of false transitions. The location of GlyR-QDs along the trajectory (Fig. 6*A4*) was determined at the end of this processing.

After 1 h of treatment with latrunculin or nocodazole, the number of transitions between the synaptic and extrasynaptic compartments was 2.4 and 2.5 times higher than in control conditions, respectively (Fig. 6*B*) ($n_{\text{recordingCtr}} = 10$; $n_{\text{recordingLat}} = 12$; $n_{\text{recordingNz}} = 8$; 13 ± 1 GlyR-QDs by recording; Lat, $p < 0.01$; Nz, $p < 0.05$; Mann–Whitney test). The increase in transition number was associated with a 4- and 5.4-fold decrease in the mean dwell time of GlyRs at synapses in the presence of latrunculin and nocodazole, respectively (Fig. 6*C*) (Lat, $p < 0.05$; Nz, $p < 0.05$; Mann–Whitney test). Because no change in FM4-64 staining was noted, which is consistent with the independence of F-actin of synaptic vesicle clusters (Sankaranarayanan et al., 2003), these effects were not attributable to changes in the number of synapses. Our results establish that actin and microtubules control GlyR exchanges between the synaptic and extrasynaptic compartments and GlyR dwell times at synapses.

We then compared the time course of latrunculin and nocodazole effects on GlyR diffusion with those seen in immunofluorescence. The maximum effect on the transitions between the compartments and dwell time at synapses was reached 4–10 min after the addition of the drugs (Fig. 6*D*). These effects on GlyR lateral dynamics were concomitant with those seen for GlyR cluster-associated fluorescence at synapses, which was already significantly decreased 5 min after the addition of the drugs (Fig. 2*B1*). Our data correlate the regulation of receptor number at synapses with receptor flux and dwell time at synapses.

Distinct effects of F-actin and mictrotubule disruption on GlyR diffusion coefficients and confinement at synapses

We then analyzed the effects of latrunculin and nocodazole treatments on GlyR diffusive behavior. We plotted the MSD as a function of time, which provides information on diffusive behavior (brownian, directed, or confined) and diffusion coefficients (references in Saxton and Jacobson, 1997). Diffusion coefficients and confinement were calculated from parts of trajectories (30–150 frames) during which QDs remained in the same compartment and did not blink. For the analyses of diffusion coefficients, because of the large dispersal of the values (over four orders of magnitude), we compared the distributions rather than the mean values.

GlyRs were tracked in Vege-transfected neurons at identified inhibitory synapses (FM staining apposed and Vege-containing

areas) (Fig. 5) and in nontransfected neurons in the synaptic and extrasynaptic compartments. The MSD versus time curves of GlyR-QDs tracked at identified inhibitory contacts in transfected neurons and at unidentified synapses in nontransfected neurons were superimposable (Fig. 7*A*). The mean diameter of the domain of confinement (d_{conf}) (Fig. 7*B*) and the diffusion coefficients (D) (Fig. 7*C1*) at FM-stained synapses in nontransfected neurons did not differ from what was found at inhibitory synapses in Vege-transfected neurons (nontransfected neurons: $n = 90$, $D_{median} = 0.001\ \mu m^2 \cdot s^{-1}$, $d_{conf} = 166 \pm 19$ nm; Vege-transfected neurons: $n = 33$, $D_{median} = 0.001\ \mu m^2 \cdot s^{-1}$, $d_{conf} = 159 \pm 35$ nm). These results support the notion that GlyRs tracked at FM4-64-stained synapses were mainly located at inhibitory synapses. This is consistent with (1) the predominance of inhibitory contacts on spinal cord neurons (Dumoulin et al., 1999) and (2) the low probability of finding GlyRs at excitatory synapses where they are not accumulated (Dumoulin et al., 2000).

Pharmacological experiments were performed on nontransfected neurons. At synapses, latrunculin induced a marked change in GlyR diffusive behavior, as illustrated by the average MSD versus time curves (Fig. 7*A*). Latrunculin treatment induced a large decrease in the confinement corresponding to an increase in the explored surface area. The mean diameter of the domain of confinement increased from 166 ± 19 to 305 ± 24 nm (Fig. 7*B*). This was consistently accompanied by an increase in the diffusion coefficients, which was reflected by a 10-fold increase in the median diffusion coefficient (Fig. 7*C1*) (control: $D_{median} = 0.001\ \mu m^2 \cdot s^{-1}$; Lat: $D_{median} = 0.01\ \mu m^2 \cdot s^{-1}$, $n = 173$; $p < 10^{-4}$, Kolmogorov–Smirnov test). It is noticeable that diffusion coefficients $<10^{-3}\ \mu m^2 \cdot s^{-1}$ were not concerned in this increase. The latrunculin-resistant GlyR-QDs may correspond to the pool of GlyRs whose associated fluorescence was not affected with the same treatments (Fig. 2*A1*,*B1*). This strong effect seen on the more rapid GlyR-QDs was reversed on removal of the drug ($D_{median} = 0.002\ \mu m^2 \cdot s^{-1}$) (supplemental Fig. 1*A1*, available at www.jneurosci.org as supplemental material). The nocodazole treatment affected neither the confinement (Fig. 7*B*) ($d_{conf} = 227 \pm 19$ nm) nor the diffusion coefficients (Fig. 7*C1*) ($D_{median} = 0.002\ \mu m^2 \cdot s^{-1}$; $n = 51$) at synapses. This absence of effects of nocodazole contrasts with the observed rapid passages of GlyR-QDs through synapses. It may be attributable to our analyses of diffusion at synapses in which short trajectories (< to 30 frames) were excluded because they do not allow reliable analyses of the MSD. In the extrasynaptic membrane (Fig. 7*C2*), latrunculin also shifted the distribution of diffusion coefficients but to a lesser extent than what was seen at synapses (control: $D_{median} = 0.007\ \mu m^2 \cdot s^{-1}$; Lat: $D_{median} = 0.02\ \mu m^2 \cdot s^{-1}$). In contrast, nocodazole induced a pronounced increase in diffusion coefficients: the median diffusion coefficient reached 0.1 $\mu m^2 \cdot s^{-1}$, which was 14 times faster than in control conditions (Fig. 7*C2*) (control: $n_{Ctr} = 231$; Lat: $n_{Lat} = 476$, $p < 10^{-4}$; Nz: $n_{Nz} = 268$; $p < 10^{-4}$, Kolmogorov–Smirnov test). These effects were also reversed on drug removal (Lat: $D_{median} = 0.007\ \mu m^2 \cdot s^{-1}$; Nz: $D_{median} = 0.004\ \mu m^2 \cdot s^{-1}$) (supplemental Fig. 1*A2*,*B*, respectively, available at www.jneurosci.org as supplemental material).

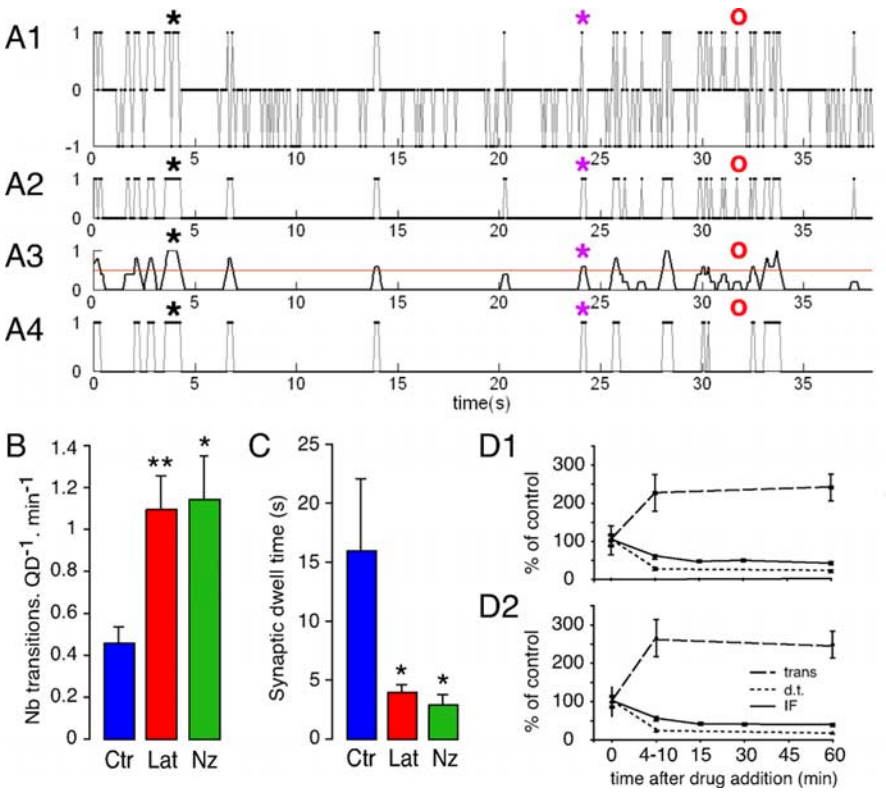

Figure 6. Effects of latrunculin and nocodazole on transitions between the compartments and dwell times at synapses. ***A***, Processing of single GlyR-QD reconstructed trajectories: example in latrunculin conditions. *x*-axis, Recording time (in seconds). *y*-axis, QD state: 1, synaptic; 0, extrasynaptic; −1, nonemitting. ***A1***, State of the GlyR-QD plotted as a function of time from a 13 Hz recording. ***A2***, State of the GlyR-QD after blink removal and time reallocation. ***A3***, Filtering of GlyR-QD transitions between the synaptic and extrasynaptic locations. The red line ($y = 0.5$) corresponds to the criteria chosen to remove artificial transitions attributable to pixelization of the FM image. ***A4***, Resulting location of the GlyR-QD. The black and purple stars indicate nonemitting events in which zero or one transition is estimated, respectively. The red circles indicate an example in which filtering attenuates the number transitions. The dwell times and number of transitions are determined after this processing. ***B***, Increased number of transitions between the synaptic and extrasynaptic compartments after Lat (red) and Nz (green) treatments compared with control conditions (Ctr) (blue). ***C***, Decreased dwell time at synapses after latrunculin and nocodazole treatment. ***D***, Latrunculin (***D1***) and nocodazole (***D2***) effects on transitions between the synaptic and extrasynaptic compartments (trans) (dashed line) and dwell time at synapses (d.t.) (dotted line) compared with fluorescence intensity of GlyR synaptic clusters (IF) (full line). The intermediate time for transitions and dwell time at synapses corresponds to the average of 9 recordings in latrunculin and 12 in nocodazole conditions acquired 4–10 min after the addition of the drug. Note that drug effects on single GlyR-QD dynamics and GlyR synaptic levels are rapid and concomitant. All data are from two independent cultures. Values are mean ± SEM. Statistical analyses: $*p < 5 \times 10^{-2}$, $**p < 10^{-2}$, $***p < 10^{-3}$; dwell times and transitions: Mann–Whitney test; fluorescence intensity: ANOVA, PLSD test.

Discussion

We have characterized the involvement of the cytoskeleton in the control of GlyR lateral diffusion. Using SPT, we found that actin and microtubules predominantly reduce diffusion in the synaptic and extrasynaptic compartments, respectively. Moreover, disruption of actin and microtubules increased GlyR exchanges between the syn-

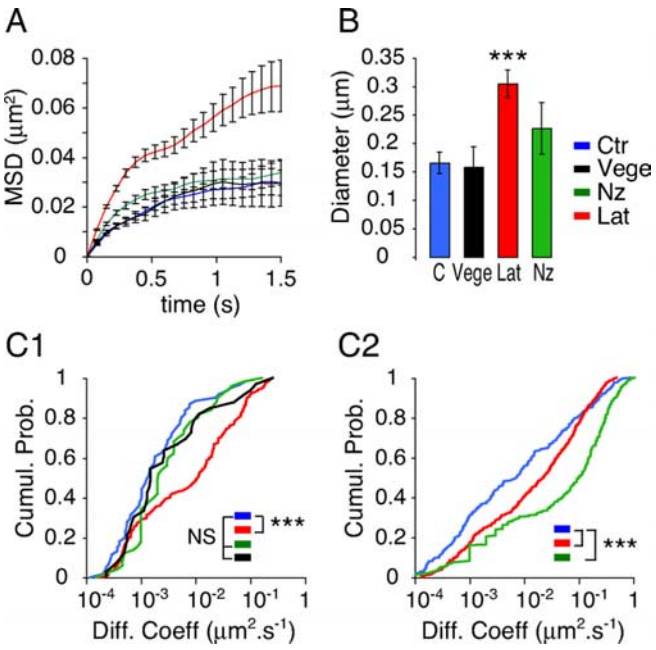

Figure 7. Distinct effects of latrunculin and nocodazole on GlyR diffusion coefficients and confinement at synapses. ***A***, Averaged MSD as a function of time of GlyR-QDs at synapses in control (Ctr) (blue), Lat (red), or Nz (green) conditions. The black curve corresponds to GlyR-QDs tracked on neurons transfected with Vege chimera at identified inhibitory synapses. Values are mean ± SEM. ***B***, Size of the domain of confinement at synapses (mean ± SEM). Latrunculin but not nocodazole treatment decreased the confinement. $^{***}p < 10^{-3}$, ANOVA, PLSD test. ***C***, Cumulative probabilities of GlyR-QD diffusion coefficients when tracked in the synaptic (***C1***) or extrasynaptic membrane (***C2***). Latrunculin and nocodazole treatments have the greatest effects in the synaptic and extrasynaptic compartments, respectively. Note the similarity between GlyR-QD diffusive behavior at FM4-64-stained synapses in nontransfected neurons (blue) and at inhibitory synapses in Vege-transfected neurons (black). Five, three, and two independent cultures were analyzed for untreated cells, drug-treated cells, and Vege-transfected cells, respectively. $^{***}p < 10^{-3}$; NS, not significant, Kolmogorov–Smirnov test.

aptic and extrasynaptic compartments and decreased receptor dwell time at synapses. These changes in GlyR diffusion were concomitant with a decrease in GlyR number at synapses, which was associated with lower gephyrin levels at synapses.

Control of lateral diffusion in the plasma membrane

SPT allows investigation of plasma membrane organization. Most SPT studies have been performed in non-neuronal cells. They have led to the model in which lateral diffusion is constrained by the submembrane skeleton that creates "fences" and anchors "transmembrane protein pickets" (references in Kusumi et al., 2005). However, little is known about the organization of the submembrane cytoskeleton in neurons. Here, we found that actin controls diffusion at synapses, whereas both actin and microtubules control diffusion in the extrasynaptic membrane. This is consistent with an early ultrastructural study by Gulley and Reese (1981), which reports that microfilaments belong to a large cortical meshwork and are concentrated beneath excitatory and inhibitory postsynaptic membranes, just below the postsynaptic scaffold. Microtubules are often enmeshed within the microfilaments but not specifically concentrated at postsynaptic sites. Direct contacts between the cytoskeleton and the plasma membrane were observed at extrasynaptic locations (Gulley and Reese, 1981). Moreover, the major effect of nocodazole on GlyR lateral diffusion in the extrasynaptic compartment supports the idea that the submembrane microtubule network is crucial in the control of the "apparent viscosity" of the neuronal membrane and might be quite dynamic, as seen in polarized epithelial cells (Reilein and Nelson, 2005).

We observed that the increase in GlyR diffusion after cytoskeleton disruption was associated with an increase in the exchanges between the synaptic and extrasynaptic compartments. Increased GlyR mobility in the extrasynaptic membrane raises the probability of entering a synapse, whereas increased GlyR mobility inside synapses raises the probability of exiting from a synapse. Interestingly, increased neuronal activation accelerates the lateral mobility of AMPA receptors in the extrasynaptic membrane (Groc et al., 2004), whereas a protocol of chemical long-term depression, known to reduce synaptic receptor number, leads to increased diffusion of AMPA receptors inside synapses (Tardin et al., 2003). Thus, modulation of the "apparent viscosity" of the membrane because of rapid remodeling of the submembrane skeleton could be a way to control the "influx" and "efflux" of receptors at synapses.

Cytoskeleton and receptor stabilization at synapses

Receptor stabilization at synapses is crucial in determining the equilibrium between the pools of synaptic and extrasynaptic receptors. Actin and microtubules can regulate GlyR stabilization at synapses at many levels and by distinct mechanisms. This regulation involves (1) the avidity of the postsynaptic scaffold for receptors; (2) molecule crowding that relies on the density of receptors, which act as pickets in the synapses, and on the submembrane accumulation of proteins, which exert a global corralling effect on receptors; and likely (3) adhesion molecules, which create permeable barriers at the edge of excitatory and inhibitory synapses (Triller and Choquet, 2003) and depend on both actin (Juliano, 2002; Yamagata et al., 2003; Bamji, 2005) and microtubules (Barth et al., 1997; Schoenwaelder and Burridge, 1999). Disruption of F-actin and microtubules leads to comparable decreases in both GlyR levels and dwell time at synapses. However, the two types of disruption affect GlyR diffusion at synapses differently. F-actin disruption increased GlyR diffusion coefficients inside synapses and the mean diameter of the domain of confinement to 305 ± 24 nm, a size comparable with that of inhibitory postsynaptic differentiations (Colin et al., 1998). In contrast, after microtubule disruption, despite short and rapid passages of GlyR-QDs through synapses, there were no significant changes in GlyR diffusion at synapses. Furthermore, differences in receptor mobility at synapses were observed with latrunculin and nocodazole treatments, despite similar amounts of gephyrin. Nonetheless, these treatments have different effects on gephyrin cluster dynamics (Hanus et al., 2006). This suggests that gephyrin cluster dynamics contribute to the avidity of the postsynaptic scaffold for receptors, in addition to the number of binding sites available for receptors.

Importantly, we found a pool of GlyRs resistant to the disruption of the cytoskeleton in both immunofluorescence and SPT experiments. In SPT, this pool corresponded to the slowest synaptic receptors (diffusion coefficients $<10^{-3}$ $\mu m^2 \cdot s^{-1}$) and represented ~30% of the receptors tracked at synapses. This suggests that the stabilization of a population of very slow synaptic GlyRs is strong and insensitive to cytoskeleton disruption. This population might be important, in situations of important plastic or pathologic cytoskeleton remodeling, in limiting fluctuations in synaptic receptor number, and in stabilizing the synapse with a basal level of neurotransmission.

Receptor lateral diffusion and receptor level at synapses

Receptor number at synapses is one of the main determinants of synaptic strength and undergoes fluctuations in the most common forms of synaptic plasticity. We found here that the maintenance of GlyR and gephyrin levels at synapses is controlled by actin and microtubules. This is consistent with the direct interaction of gephyrin with polymerized tubulin (Kirsch et al., 1991) and actin-regulating proteins (Mammoto et al., 1998; Kins et al., 2000; Giesemann et al., 2003). It is also compatible with previous studies indicating that F-actin disruption decreases the size of gephyrin clusters (Kirsch and Betz, 1995), and that microtubule disruption generates a loss of gephyrin and the lateral spread of GlyRs from synapses in spinal cord neurons (Kirsch and Betz, 1995; van Zundert et al., 2004). Our quantitative analyses revealed that, during cytoskeleton depolymerization, GlyR-associated fluorescence diminished within a few minutes and before gephyrin-associated fluorescence. This suggests that GlyRs leave synapses before the disruption of the gephyrin-based subsynaptic scaffold and that a cytoskeleton-dependent process modulates within minutes the time it takes for a receptor to exit a synapse. These data support the notion that, whereas the accumulation of inhibitory receptors at synapses relies on gephyrin (Kirsch et al., 1993; Essrich et al., 1998; Feng et al., 1998; Kneussel et al., 1999; Levi et al., 2004; Jacob et al., 2005), receptors may also help stabilize the cytoplasmic protein gephyrin below the subsynaptic membrane. This is compatible with the notion that, independently of the local turnover of the constitutive elements of the synapse, reciprocal interactions within the postsynaptic differentiation are crucial for the stability of a synaptic contact. Furthermore, the decrease in GlyR level at synapses was concomitant with a decrease in receptor dwell time at synapses and with an increase in receptor exchanges between the synaptic and extrasynaptic compartments. This suggests that, whereas long-term regulations of synaptic strength are coupled to global remodeling of the postsynaptic scaffold (McGee and Bredt, 2003; Collingridge et al., 2004; Perez-Otano and Ehlers, 2005), changes in receptor number at synapses on short timescales can result from changes in receptor flux at synapses.

Excitatory neurotransmission has been shown to regulate inhibitory neurotransmission, gephyrin cluster size and dynamics (Gonzalez-Forero et al., 2005; Hanus et al., 2006), and, through an action on the cytoskeleton, diffusion in the plasma membrane (Richards et al., 2004). At the cellular level, cytoskeleton-regulating proteins, such as profilin, Mena/VASP, or GDP/GTP exchange factors, which also regulate microtubules dynamics (Gundersen et al., 2004), are components of both inhibitory (Kins et al., 2000; Giesemann et al., 2003) and excitatory (Dillon and Goda, 2005) postsynaptic differentiations and ubiquitous components of the submembrane cytoskeleton cortex. Some of these proteins are regulated by synaptic activity (Ackermann and Matus, 2003; Lamprecht and LeDoux, 2004; Oertner and Matus, 2005) and may be involved in the activity-dependent regulations of actin dynamics (Star et al., 2002; Oertner and Matus, 2005), which differ between dendritic spines and the dendritic shaft during synaptic plasticity (Furuyashiki et al., 2002). Thus, depending on the extracellular cues, the submembrane cytoskeleton might be regulated (1) globally in the extrasynaptic compartment, leading to changes in receptor influx at synapses, and/or (2) locally at synapses, with consequences for postsynaptic differentiation properties and thereby for receptor stabilization.

In conclusion, our data demonstrate that GlyR exchanges between the synaptic and extrasynaptic membranes and GlyR stabilization at synapses can be regulated in response to actin or microtubule cytoskeleton remodeling, and can change receptor number at synapses. Modulations of the submembrane cytoskeleton, in relation to synaptic activity, may have various consequences for the dynamics of the receptor/scaffold complexes. Considering the synapse as a self-organized structure, whose plasticity relies on the transient nature of the interactions among its components (Misteli, 2001), it will be important to characterize the collective dynamics of receptor and scaffolding molecules and how they are regulated.

References

Ackermann M, Matus A (2003) Activity-induced targeting of profilin and stabilization of dendritic spine morphology. Nat Neurosci 6:1194–1200.

Adesnik H, Nicoll RA, England PM (2005) Photoinactivation of native AMPA receptors reveals their real-time trafficking. Neuron 48:977–985.

Alivisatos AP, Gu W, Larabell C (2005) Quantum dots as cellular probes. Annu Rev Biomed Eng 7:55–76.

Allison DW, Gelfand VI, Spector I, Craig AM (1998) Role of actin in anchoring postsynaptic receptors in cultured hippocampal neurons: differential attachment of NMDA versus AMPA receptors. J Neurosci 18:2423–2436.

Bamji SX (2005) Cadherins: actin with the cytoskeleton to form synapses. Neuron 47:175–178.

Barth AI, Nathke IS, Nelson WJ (1997) Cadherins, catenins and APC protein: interplay between cytoskeletal complexes and signaling pathways. Curr Opin Cell Biol 9:683–690.

Becker CM, Hoch W, Betz H (1988) Glycine receptor heterogeneity in rat spinal cord during postnatal development. EMBO J 7:3717–3726.

Bonneau S, Cohen L, Dahan M (2004) A multiple target approach for single quantum dot tracking. Proceeding of the IEEE International Symposium on Biological Imaging, Arlington, VA, April.

Choquet D, Triller A (2003) The role of receptor diffusion in the organization of the postsynaptic membrane. Nat Rev Neurosci 4:251–265.

Colin I, Rostaing P, Augustin A, Triller A (1998) Localization of components of glycinergic synapses during rat spinal cord development. J Comp Neurol 398:359–372.

Collingridge GL, Isaac JT, Wang YT (2004) Receptor trafficking and synaptic plasticity. Nat Rev Neurosci 5:952–962.

Dahan M, Levi S, Luccardini C, Rostaing P, Riveau B, Triller A (2003) Diffusion dynamics of glycine receptors revealed by single-quantum dot tracking. Science 302:442–445.

Dillon C, Goda Y (2005) The actin cytoskeleton: integrating form and function at the synapse. Annu Rev Neurosci 28:25–55.

Dumoulin A, Rostaing P, Bedet C, Levi S, Isambert MF, Henry JP, Triller A, Gasnier B (1999) Presence of the vesicular inhibitory amino acid transporter in GABAergic and glycinergic synaptic terminal boutons. J Cell Sci 112:811–823.

Dumoulin A, Levi S, Riveau B, Gasnier B, Triller A (2000) Formation of mixed glycine and GABAergic synapses in cultured spinal cord neurons. Eur J Neurosci 12:3883–3892.

Essrich C, Lorez M, Benson JA, Fritschy JM, Luscher B (1998) Postsynaptic clustering of major $GABA_A$ receptor subtypes requires the γ2 subunit and gephyrin. Nat Neurosci 1:563–571.

Feng G, Tintrup H, Kirsch J, Nichol MC, Kuhse J, Betz H, Sanes JR (1998) Dual requirement for gephyrin in glycine receptor clustering and molybdoenzyme activity. Science 282:1321–1324.

Furuyashiki T, Arakawa Y, Takemoto-Kimura S, Bito H, Narumiya S (2002) Multiple spatiotemporal modes of actin reorganization by NMDA receptors and voltage-gated Ca^{2+} channels. Proc Natl Acad Sci USA 99:14458–14463.

Giesemann T, Schwarz G, Nawrotzki R, Berhorster K, Rothkegel M, Schluter K, Schrader N, Schindelin H, Mendel RR, Kirsch J, Jockusch BM (2003) Complex formation between the postsynaptic scaffolding protein gephyrin, profilin, and Mena: a possible link to the microfilament system. J Neurosci 23:8330–8339.

Gonzalez-Forero D, Pastor AM, Geiman EJ, Benitez-Temino B, Alvarez FJ (2005) Regulation of gephyrin cluster size and inhibitory synaptic currents on Renshaw cells by motor axon excitatory inputs. J Neurosci 25:417–429.

Groc L, Heine M, Cognet L, Brickley K, Stephenson FA, Lounis B, Choquet D

(2004) Differential activity-dependent regulation of the lateral mobilities of AMPA and NMDA receptors. Nat Neurosci 7:695–696.
Gulley RL, Reese TS (1981) Cytoskeletal organization at the postsynaptic complex. J Cell Biol 91:298–302.
Gundersen GG, Gomes ER, Wen Y (2004) Cortical control of microtubule stability and polarization. Curr Opin Cell Biol 16:106–112.
Hanus C, Ehrensperger MV, Triller A (2006) Activity-dependent movements of postsynaptic scaffolds at inhibitory synapses. J Neurosci 26:4586–4595.
Jacob TC, Bogdanov YD, Magnus C, Saliba RS, Kittler JT, Haydon PG, Moss SJ (2005) Gephyrin regulates the cell surface dynamics of synaptic $GABA_A$ receptors. J Neurosci 25:10469–10478.
Juliano RL (2002) Signal transduction by cell adhesion receptors and the cytoskeleton: functions of integrins, cadherins, selectins, and immunoglobulin-superfamily members. Annu Rev Pharmacol Toxicol 42:283–323.
Kins S, Betz H, Kirsch J (2000) Collybistin, a newly identified brain-specific GEF, induces submembrane clustering of gephyrin. Nat Neurosci 3:22–29.
Kirsch J, Betz H (1995) The postsynaptic localization of the glycine receptor-associated protein gephyrin is regulated by the cytoskeleton. J Neurosci 15:4148–4156.
Kirsch J, Langosch D, Prior P, Littauer UZ, Schmitt B, Betz H (1991) The 93-kDa glycine receptor-associated protein binds to tubulin. J Biol Chem 266:22242–22245.
Kirsch J, Wolters I, Triller A, Betz H (1993) Gephyrin antisense oligonucleotides prevent glycine receptor clustering in spinal neurons. Nature 366:745–748.
Kneussel M, Hermann A, Kirsch J, Betz H (1999) Hydrophobic interactions mediate binding of the glycine receptor β-subunit to gephyrin. J Neurochem 72:1323–1326.
Kusumi A, Sako Y (1996) Cell surface organization by the membrane skeleton. Curr Opin Cell Biol 8:566–574.
Kusumi A, Sako Y, Yamamoto M (1993) Confined lateral diffusion of membrane receptors as studied by single particle tracking (nanovid microscopy). Effects of calcium-induced differentiation in cultured epithelial cells. Biophys J 65:2021–2040.
Kusumi A, Nakada C, Ritchie K, Murase K, Suzuki K, Murakoshi H, Kasai RS, Kondo J, Fujiwara T (2005) Paradigm shift of the plasma membrane concept from the two-dimensional continuum fluid to the partitioned fluid: high-speed single-molecule tracking of membrane molecules. Annu Rev Biophys Biomol Struct 34:351–378.
Lamprecht R, LeDoux J (2004) Structural plasticity and memory. Nat Rev Neurosci 5:45–54.
Levi S, Vannier C, Triller A (1998) Strychnine-sensitive stabilization of postsynaptic glycine receptor clusters. J Cell Sci 111:335–345.
Levi S, Logan SM, Tovar KR, Craig AM (2004) Gephyrin is critical for glycine receptor clustering but not for the formation of functional GABAergic synapses in hippocampal neurons. J Neurosci 24:207–217.
Mammoto A, Sasaki T, Asakura T, Hotta I, Imamura H, Takahashi K, Matsuura Y, Shirao T, Takai Y (1998) Interactions of drebrin and gephyrin with profilin. Biochem Biophys Res Commun 243:86–89.
McGee AW, Bredt DS (2003) Assembly and plasticity of the glutamatergic postsynaptic specialization. Curr Opin Neurobiol 13:111–118.
Meier J, Vannier C, Serge A, Triller A, Choquet D (2001) Fast and reversible trapping of surface glycine receptors by gephyrin. Nat Neurosci 4:253–260.
Misteli T (2001) The concept of self-organization in cellular architecture. J Cell Biol 155:181–185.
Moss SJ, Smart TG (2001) Constructing inhibitory synapses. Nat Rev Neurosci 2:240–250.
Nagai T, Ibata K, Park ES, Kubota M, Mikoshiba K, Miyawaki A (2002) A variant of yellow fluorescent protein with fast and efficient maturation for cell-biological applications. Nat Biotechnol 20:87–90.
Oertner TG, Matus A (2005) Calcium regulation of actin dynamics in dendritic spines. Cell Calcium 37:477–482.
Perez-Otano I, Ehlers MD (2005) Homeostatic plasticity and NMDA receptor trafficking. Trends Neurosci 28:229–238.
Prior P, Schmitt B, Grenningloh G, Pribilla I, Multhaup G, Beyreuther K, Maulet Y, Werner P, Langosch D, Kirsch J, Betz H (1992) Primary structure and alternative splice variants of gephyrin, a putative glycine receptor-tubulin linker protein. Neuron 8:1161–1170.
Ransom BR, Christian CN, Bullock PN, Nelson PG (1977) Mouse spinal cord in cell culture. II. Synaptic activity and circuit behavior. J Neurophysiol 40:1151–1162.
Reilein A, Nelson WJ (2005) APC is a component of an organizing template for cortical microtubule networks. Nat Cell Biol 7:463–473.
Richards DA, De Paola V, Caroni P, Gahwiler BH, McKinney RA (2004) AMPA-receptor activation regulates the diffusion of a membrane marker in parallel with dendritic spine motility in the mouse hippocampus. J Physiol (Lond) 558:503–512.
Sankaranarayanan S, Atluri PP, Ryan TA (2003) Actin has a molecular scaffolding, not propulsive, role in presynaptic function. Nat Neurosci 6:127–135.
Saxton MJ (1997) Single-particle tracking: the distribution of diffusion coefficients. Biophys J 72:1744–1753.
Saxton MJ, Jacobson K (1997) Single-particle tracking: applications to membrane dynamics. Annu Rev Biophys Biomol Struct 26:373–399.
Schoenwaelder SM, Burridge K (1999) Bidirectional signaling between the cytoskeleton and integrins. Curr Opin Cell Biol 11:274–286.
Star EN, Kwiatkowski DJ, Murthy VN (2002) Rapid turnover of actin in dendritic spines and its regulation by activity. Nat Neurosci 5:239–246.
Tardin C, Cognet L, Bats C, Lounis B, Choquet D (2003) Direct imaging of lateral movements of AMPA receptors inside synapses. EMBO J 22:4656–4665.
Thomas P, Mortensen M, Hosie AM, Smart TG (2005) Dynamic mobility of functional $GABA_A$ receptors at inhibitory synapses. Nat Neurosci 8:889–897.
Tovar KR, Westbrook GL (2002) Mobile NMDA receptors at hippocampal synapses. Neuron 34:255–264.
Triller A, Choquet D (2003) Synaptic structure and diffusion dynamics of synaptic receptors. Biol Cell 95:465–476.
Turrigiano GG, Nelson SB (2004) Homeostatic plasticity in the developing nervous system. Nat Rev Neurosci 5:97–107.
van Zundert B, Alvarez FJ, Tapia JC, Yeh HH, Diaz E, Aguayo LG (2004) Developmental-dependent action of microtubule depolymerization on the function and structure of synaptic glycine receptor clusters in spinal neurons. J Neurophysiol 91:1036–1049.
Yamagata M, Sanes JR, Weiner JA (2003) Synaptic adhesion molecules. Curr Opin Cell Biol 15:621–632.
Zhang W, Benson DL (2001) Stages of synapse development defined by dependence on F-actin. J Neurosci 21:5169–5181.